Aquat. Sci.
DOI 10.1007/s00027-005-0750-0

Aquatic Sciences

Research Article

Spatial models as a tool to identify spatial patterns of surficial sediment composition and their contributing factors in the littoral zone of Lake Constance (Germany)

Klaus Schmieder [1,*], Hans-Peter Piepho [2] and Heinz G. Schröder [3]

[1] Institute of Landscape and Plant Ecology, University of Hohenheim, D-70593 Stuttgart, Germany
[2] Institute of Crop Production and Grassland Research, University of Hohenheim, D-70593 Stuttgart, Germany
[3] Institute of Lake Research of the Environmental Protection Agency Baden-Württemberg, D-88085 Langenargen, Germany

Received: 16 April 2004; revised manuscript accepted: 24 March 2005

Abstract. For a lake-wide investigation of littoral surface sediments, we collected approximately 800 samples from Lake Constance along 235 parallel transects of 1 km distance along the shore at water depths of 1, 2, 4 and 8 m. Sediment samples were analyzed for the presence of spatial patterns in mineralogical and granulometric composition and contents of carbon and sulphur, with the purpose of identifying general and lake specific processes that contribute to the observed patterns. In particular, we wanted to test if the general factors known for contributing to littoral sediment composition could be revealed by spatial modeling of a dataset based on a systematic sampling scheme. Explanatory variables for a regression model were derived from GIS-analyses of the dataset, and also from other available data on Lake Constance. Highest levels of variance explained by the model (30–40%) were reached for the parameters calcite, clay minerals, sulphur and inorganic carbon content. Regional patterns in sediment composition, described by the proportion of explained between-transect variance (VE_t) in the model, are explained by up to 70%. The observed east-west gradient of mineralogical sediment composition is ascribed to the respective regional patterns of allogenic and endogenic sources. Allogenic minerals such as clay, dolomite and quartz dominate the littoral surface sediments of the eastern part of the lake and the areas near river mouths. Endogenic minerals like calcite dominate the littoral sediments of the western parts of the lake, reflecting internal process of biogenic carbonate precipitation that corresponds to the distribution patterns of submersed macrophytes (particularly Charophytes).

This study confirms the major factors contributing to littoral sediment composition found in previous studies. However, their explanatory power for spatial patterns of a specific lake will be weak if respective spatial patterns of influence are neglected. The present study provides a guide to future sampling schemes and corresponding spatial statistics for lake specific application of general models. It also provides a basis to support engineering decisions for specific lake development.

Key words. Littoral sediments; mineralogy; granulometry; linear regression modeling.

Introduction

Littoral sediment composition is determined by the geological composition of the drainage area, morphological features of the shoreline and biological, physical as well as chemical processes in lakes. According to the source, min-

* Corresponding author phone: ++49 711 4593608;
fax: ++49 711 4592831; e-mail: schmied@uni-hohenheim.de
Published Online First: ■

erals can be classified as allogenic, endogenic and authigenic (Jones and Bowser, 1978). Littoral surface sediments are influenced by external processes such as river transport from the catchment (Müller, 1966a). Effect of river input may differ substantially depending upon both the rate of discharge and the relative quantities of bed and suspended load (Sly, 1978). Non-clay clastic minerals consisting principally of quartz and feldspar reflect sediment source and transport, and contribute mainly to the allogenic sediment fraction. These minerals are particularly useful for determination of source and the evaluation of physical processes within a lake (Jones and Bowser, 1978).

Carbonate minerals constitute another important fraction of many lake sediments. They can derive in significant quantities from all three sediment sources (Jones and Bowser, 1978; Kelts and Hsü, 1978). Limestone detritus in Alpine alluvial fans and in the Molasse beds of adjacent regions, can account in large part for the carbonate sediments of prealpine lakes (Müller, 1966a). Internal lake processes such as accumulation of mollusc shells (Brown et al., 1992), calcite precipitation from pelagic algae (Küchler-Krischun, 1989) or littoral macrophytes (Schöttle, 1969; Jones and Bowser, 1978; Kelts and Hsü, 1978; Schröder, 1982) contribute to the endogenic sediment fraction. Littoral macrophytes also contribute to the organic fraction of littoral sediments indicated by organic carbon and sulphur content. Anaerobic conditions associated with organic decay, promote the development of H_2S as well as iron reduction, and facilitate the genesis of pyrite minerals (Jones and Bowser, 1978).

The spatial distribution of littoral sediment components is modified by shore erosion and transport by wave action (Sly, 1978; Jones and Bowser, 1978; Petticrew and Kalff, 1991). For instance, the decay of organic matter produced in the littoral zone only takes place in protected littoral areas; in exposed areas, it is transported onshore or to deeper parts of a lake. Influence of waves is determined by the effects of fetch, duration, incidence, and bathymetry. Sediment response to the imposed shear stress is itself controlled by grain size, cohesive strength, and bed form (Sly, 1978). The occurrence of sorted course sands and gravels is largely confined to shallow water areas (Sly, 1978). Beaches and other areas subject to strong current action favor the resistant minerals, chiefly quartz; whereas the accumulation of organic material, clay or precipitate minerals takes place under relatively static conditions (Jones and Bowser, 1978). Macrophytes affect granulometric composition by reducing currents and wave action during the growing season, thereby facilitating particle sedimentation (Schröder, 1988; James and Barko, 1990) and the protection of shore areas from erosion (Schröder, 1982; Vermaat et al., 2000). The relative importance of endogenic and allogenic processes might be estimated by the quantitative mineralogy of sediments (Jones and Bowser, 1978).

The scope of this study was to provide a detailed overview of littoral surface sediment composition of Lake Constance on a regional scale and to identify general and lake specific factors and processes that contribute to the observed patterns. Littoral sediment composition was modeled previously (e.g. Petticrew and Kalff, 1991), so that general factors contributing to sediment composition are known. However, the authors selected a relatively small number of spatially independent sample sites with a wide range of proposed variables for the model. The relative contribution of different factors to littoral sediment composition is strongly dependent on lake specific and site specific variation. Thus, lake specific applicability of these models is limited.

The present study employed a more comprehensive sampling scheme with systematic coverage of the shoreline and the respective spatial patterns in sediment composition. This scheme allows a neutral assessment of the explanatory power of different environmental variables relative to environmental variability. Moreover, we assessed the importance of different variables accounting for spatial autocorrelation, thus yielding valid significance tests. In particular, we wanted to test if the general factors known for contributing to littoral sediment composition could be revealed on the basis of a systematic sampling scheme. Furthermore, the contribution of major variables to the observed variance in sediment composition was evaluated, thus providing a better understanding of the processes in the littoral zone of Lake Constance. By including spatial variables in the models and allowing for spatial autocorrelation, the regional differences in the influence of sediment constituting variables can be detected. In addition, this study served as a basis to investigate factors explaining the spatial distribution of submersed macropyhtes done by Schmieder and Lehmann (2004).

Study area

Lake Constance is the second largest prealpine European lake next to Lake Geneva. The lake is traditionally divided into an Upper Lake and a Lower Lake (Fig. 1). The water body is strongly affected by wind-action, with strong winds mainly coming from the southwest (Mühleisen, 1977). This pattern contributes to the presence of extended littoral areas exposed to this wind direction. Lake Constance is a phosphorus-limited, mesotrophic hard water lake with biogenically induced calcite precipitation. The total catchment area of 11,500 km^2 is approximately 20 times the size of its lake surface area and is distributed over three countries: Switzerland with Liechtenstein (48% of the area), Germany (28%) and Austria (24%). Over 90% of the water flow originates from the Alps and reaches the eastern part of the Upper Lake through three inflows: the Rhine River (“Alpen-

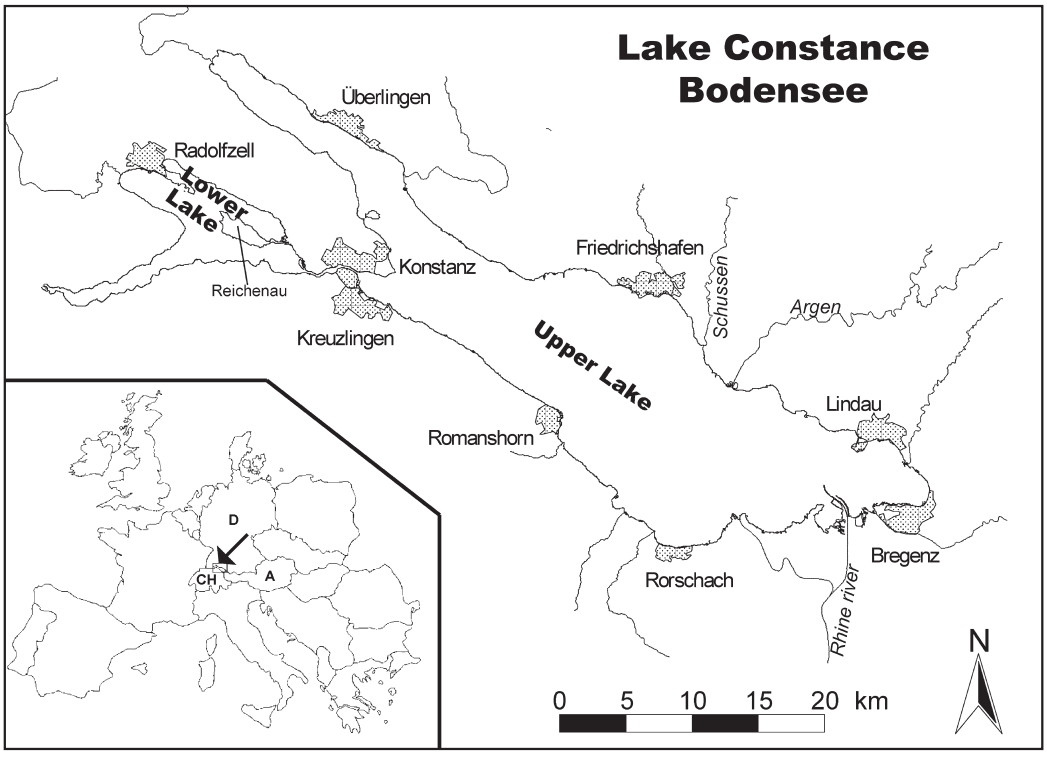

Figure 1. Map of Lake Constance with country borders (D = Germany, CH = Switzerland, A= Austria), cities and main tributaries.

rhein"), "Bregenzerach" and the "Dornbirnerach". Geologically, the lake basin is situated in the molasse basin of the northern alpine foothills and was mainly formed by water and ice activity during the last Quaternary glaciation period more than 15,000 years ago. After the withdrawal of the ice, eroded material from the alpine and subalpine catchment area entered Lake Constance through the Rhine River and smaller tributaries. Major lake deposits are gravel and suspended matter from the Mesozoic carbonates and metamorphic layers as well as tertiary sandstones from the northern alpine region.

Materials and methods

Sediment sampling

From July to September 1993, samples of the surficial sediment were taken with an Ekman-Birge sampler on 235 parallel littoral transects 1 km apart along the shore at water depths of 1, 2, 4 and 8 m. In cases where penetration of the sampler was not possible due to dense submersed macrophytes or coarse gravel, collection of sediments was attempted by snorkeling. Failure of the sampler led to missing values in the data set. Missing values also arose from shore depositions and shore constructions that, in particular, covered several sample locations at 1 m water depth. Samples were stored in sealed plastic cases in a cool box and transported to the laboratory where they were frozen until further processing.

Sediment analysis

Grain size analysis of the sand and gravel fraction were performed by gravimetrical sieve analysis with a RETSCH VE 1000 sieving machine (RETSCH, Haan, Germany) filled with 200 × 50 mm sieves according to the German laboratory standard DIN ISO-3310/1. The silt and clay fractions were identified by laser optical particle counter analysis with a GALAI CIS 1 (LOT ORIEL, Darmstadt, Germany). For detailed description of the procedure see Schmieder et al. (2004). Determination of carbon and sulphur was performed from the dried silt-clay fraction (drying temperature: 60 °C). Samples were pulverized and homogenized in a mortar mill (FRITSCH Pulverisette 2, FRITSCH, Idar-Oberstein, Germany). Mineralogical powder analysis after Debye-Scherrer (described in Müller, 1966b) was performed with a SIEMENS Kristalloflex D 500 x-ray diffractometer using an angle range of 4 to 70 degrees. By referring to the precisely measured contents of inorganic carbon, the proportion of the carbonate minerals, calcite and dolomite, could be quantitatively determined from the height of the measured reflection peaks. The amount of silicate minerals (quartz, clay minerals etc.) was semi-quantitatively described by comparing their peak heights with those of carbonate minerals.

GIS procedures

Analytical data were entered into the spreadsheet program MS Excel and integrated into the data base of a Geographic Information System (GIS, ARCGIS/ARCVIEW, ESRI Kranzberg). The Northings and Eastings of the sediment samples were obtained by intersecting the digitised transect lines with depth contour lines from the digital elevation model of the lake (Braun and Schärpf, 1994). The distance from shore of the sampling locations was automatically calculated by the GIS in the course of a spatial join operation of the datasets of the sample locations and the shoreline. The explanatory variable "abundance of *Chara contraria*" was added to the dataset by intersecting the sediment dataset with the dataset of plant distribution (Schmieder, 1997; 1998). The explanatory variable "effective fetch distance" (hereafter *EFD*) was calculated using an ARCVIEW script (Lehmann, 1998).

Statistical analysis

Data were analysed by multiple linear regression using sediment parameters as the response variables (Table 1). Mean total grain size (MEANTOT; see Table 1) was computed as (Φ16 + Φ50 + Φ84)/3, where Φp is the p-percentile of the grain weight distribution (Folk and Ward, 1957). We transformed most response variables (Table 1) to achieve approximate normality, as diagnosed by histograms. For Pyrite, we deleted two outlying observations.

The following variables were used as explanatory variables in multiple regression:

- Northings (*N*; km), standardized by subtraction of mean
- Eastings (*E*; km), standardized by subtraction of mean
- Depth below mean water surface level (m)
- Distance from shoreline (m)
- Slope = depth/distance
- *EFD* (Hakanson and Janson, 1983; in *m*; divided by 1000)
- Abundance of *Chara contraria* in two classes: Chara = 0: low abundance, Chara = 1: highly abundant

The explanatory variables were chosen to represent a suite of processes in the lake connected with sediment formation. Geographic coordinates are indirect variables that refer to general spatial trends originating from: 1) geological differences of the shore areas, 2) the location of tributaries as allogenic sources of littoral sediments, and 3) the prevailing direction of strong winds. *EFD* represents the amplitude of waves affecting the littoral surface sediments in the respective wind direction. The wave effect also depends on water depth, the distance from shore and the slope of the littoral zone. The abundance of the most common Charophyte *Chara contraria* in the littoral zone represents the endogenic process of biogenic carbonate production. The plants grow in dense meadows, thus attenuating currents and wave effects during their growth period and increasing the sedimentation rate.

Table 1. Description of sediment parameters used as response variables and statistical transformation used to linearise the data.

Label	Description	Unit	Transformation
Calcite	weight percentage	%	None
Dolomite		%	Square root
Calcite/ Dolomite		%	Log
Quartz		%	Square root
Feldspar		%	Quartic root ($x^{0.25}$)
Clay minerals (Claymin)		%	Square root
Pyrite		%	None
Sulphur (S)		%	Log
Inorganic Carbon (Can)		%	None
Organic Carbon (Corg)		%	Square root
PCLT63	weight percentage of grain size fraction <63 µm	%	Quartic root ($x^{0.25}$)
MEANLT63	mean grain size of the fraction <63 µm	µm	Square root
MEANTOT	mean total grain size	µm	Log

Observations were modelled by

$$y_{ij} = \eta(x_{ij}) + t_i + e_{ij} \quad (1)$$

where $\eta(x_{ij})$ is a linear predictor depending on a vector of explanatory variables (x_{ij}), t_i is a random effect of the i-th transect, and e_{ij} is a random error term associated with the j-th measurement on the i-th transect. To account for the spatial nature in the data, we allowed for spatial autocorrelation among all t_i effects according to the models given in Table 2. All of these models assume that the covariance, and hence the correlation, among two points i and i' decays with their spatial distance $d(i, i')$. This pattern is

Table 2. Different variance-covariance structures for random effects (t_i) depending on the distance among two sampling locations. $d(i, i')$ = Euclidean distance among two sampling locations. σ_t^2 and ρ are covariance parameters.

Name	Model for covariance among points i and i'.
Power/ Exponential	$\sigma_t^2 \rho^{d(i, i')}$
Gaussian	$\sigma_t^2 \exp(-[d(i, i')]^2/\rho^2)$
Spherical	$\sigma_t^2 \left[1 - \left(\frac{3d(i, i')}{2\rho} + \frac{[d(i, i')]^3}{2\rho^3}\right)\right]$ with $d(i, i') > \rho$

typical of spatial data and needs to be accounted for in statistical analysis to obtain valid inferences.

These models were also tested for correlations among residual error terms (e_{ij}) on the same transect. The best-fitting covariance structure was selected based on the Akaike Information Criterion (AIC). The AIC involves a penalty term for the number of parameters that avoids overfitting. A model with a small AIC-value is preferable in terms of model fit (Wolfinger, 1996). All models were fitted using the REML method (Littell et al., 1996). As a first step, we assumed that $\eta(x_{ij})$ comprised all explanatory variables, regarded t_i as a fixed effect and selected the best fitting model for e_{ij}. As a second step, we regarded t_i as random and selected the best fitting structure for t_i, assuming the structure selected for e_{ij} in the first step. As a third step, we fitted and tested regression terms based on the selected variance-covariance structures for t_i and e_{ij} using approximate Wald-tests (Wolfinger, 1996). All regression terms were tested individually by t-tests, except for the coordinates *N* and *E* which were tested simultaneously by an F-test with two denominator degrees of freedom. We retained a term when it was significant at the 5 % level. In a few cases, a term was retained when the p-value was just beyond the significance level, but the term was deemed important based on subject matter knowledge.

A multiple linear regression of a response *y* on eastings (*E*) and northings (*N*) defines a response-surface (plane) in two-dimensional space. The direction of a major trend in the response corresponds to the direction of steepest ascent on the surface in the *N*-*E*-plane. If the coordinate system is rotated to the right by an angle of α so that the axis for rotated eastings (E') coincides with the direction of the major trend direction, then the rotation angle can be shown to be

$$\alpha = \tan^{-1}\left(-\frac{\beta_N}{\beta_E}\right), \tag{2}$$

where β_E and β_N are the regression coefficients corresponding to *E* and *N*, respectively. Thus, we regressed the response on *N* and *E* and then computed the axis of major trend direction from (1). The rotated eastings and northings are given by:

$$E' = E\cos(\alpha) - N\sin(\alpha) \tag{3}$$

$$N' = E\sin(\alpha) + N\cos(\alpha) \tag{4}$$

Similarly, the regression coefficients for the rotated axis E' is

$$\beta_{E'} = \beta_E\cos(\alpha) - \beta_N\sin(\alpha) \tag{5}$$

The regression coefficient for the rotated northings is zero, when rotation is according to (1):

$$\beta_{N'} = \beta_E\sin(\alpha) + \beta_N\cos(\alpha) = 0 \tag{6}$$

The fit of a multiple linear regression model is often assessed by the coefficient of determination (R^2). This measure is not available in REML-based mixed model analysis, which involves no sum-of-squares. We assessed model fit by the reduction in the variance due to fitting the regressor variables, i.e. we compute the "variance explained" (*VE*) for random terms t_i and e_{ij} as

$$VE = \frac{\sigma^2_{without} - \sigma^2_{with}}{\sigma^2_{without}} \times 100\,\% \tag{7}$$

where σ^2 is either σ_t^2 (between-transect variance) or σ_e^2 (within-transect variance) or $\sigma_t^2 + \sigma_e^2$ (total variance). The subscript indicates whether the variance is computed based on a mixed model with or without the regressors. Variance components were estimated by REML (Littell et al., 1996). When the estimate for the numerator was negative, it was set to zero.

Results

There was little if any autocorrelation among error terms e_{ij} from the same transect. We therefore assumed independent error terms throughout. In contrast, the sharp decrease for all traits in AIC of all spatial models relative to the independent model provided strong evidence of autocorrelation for the between-transect effect t_i (Table 3). Hence, autocorrelated models for t_i were used for all traits, the particular choice depending on the value of AIC. Either the power or spherical model fared best, i.e., they showed the smallest AIC. Accounting for the spatial correlation structure is important to obtain valid tests for the explanatory variables.

The p-values of the Wald-statistics for explanatory variables showed a diverse pattern (Table 4). The Depth variable was significant for all parameters except Feldspar. *EFD* was irrelevant for mineralogical parameters with the exception of clay minerals (Claymin) and quartz, but significant for organic compounds (Corg, S) and granulometric variables (PCLT63, MEANTOT). In addition to the mineral component, clay minerals also represent the fine grain (<2 µm) fraction. The Distance variable significantly explained the values of the mineralogical parameters Calcite, Dolomite, log (C/D), Claymin and Pyrite, and the inorganic carbon content (Can) and MEANTOT. The Slope variable significantly explained only the contents of Calcite, Quartz, Can and S. Chara was found significant for the parameters Calcite, Claymin, Can and the granulometric parameters MEANLT63 and MEANTOT. The spatial variables N (northings) and E (eastings) were significant in explaining the contents of Can, Corg and S, and also the mineralogical composition, except Feldspar. N and E did not significantly explain granulometric parameters.

Table 3. AIC values of variance-covariance model for t_i, assuming errors e_{ij} are independent (selected model underlined). AIC = $LL_R - q$, where LL_R is the REML log-likelihood and q is the number of parameters in the variance-covariance model. If a parameter was estimated to be zero, q was reduced accordingly. The smaller the AIC, the better the fit of a model.

	Calcite	Dolomite	log(C/D)	Quartz	Feldspar	Claymin	Pyrite
Power/exp.	5727.7	1286.2	1752.7	1317.6	308.0	1993.5	–1221.6
Gaussian	5740.3	1291.3	1763.8	1330.8	322.2	1997.5	–1220.0
Spherical	5729.1	1285.3	1752.1	1315.6	308.5	1993.2	–1216.2
Independent	5784.9	1406.0	1859.7	1372.4	377.8	2033.5	–1214.5
	S	Can	Corg	PCLT63	MEANLT63	MEANTOT	
Power/exp.	1272.1	507.7	470.2	1479.6	1631.2	1395.1	
Gaussian	1273.1	519.8	471.8	1482.0	1639.7	1397.8	
Spherical	1271.5	516.3	470.9	1542.6	1631.1	1402.6	
Independent	1298.1	545.4	479.3	1540.7	1647.3	1412.8	

Table 4. p-values of F-statistics for explanatory variables for variance-covariance models selected for t_i in Table 3.

	df[$]	Calcite	Dolomite	log(C/D)	Quartz	Feldspar	Claymin	Pyrite
EFD	1	0.1857	0.1047	0.0697	0.0213	0.6835	0.0144	0.5669
Depth	1	<0.0001	0.0160	0.0001	0.0020	0.8482	<0.0001	<0.0001
Distance	1	0.0196	0.0164	0.0010	0.0376	0.7334	0.0171	0.0196
Slope	1	0.0238	0.8173	0.3603	0.0008	0.3231	0.0512	0.2221
Chara	1	0.0154	0.5726	0.5914	0.1936	0.5812	0.0030	0.7185
$N + E$[§]	2	0.0003	0.0264	0.0103	0.0001	0.5631	<0.0001	0.0210
	df[$]	S	Can	Corg	PCLT63	MEANLT63	MEANTOT	
EFD	1	0.0125	0.3590	0.0013	0.0028	0.0548	0.0011	
Depth	1	<0.0001	<0.0001	0.0001	<0.0001	<0.0001	<0.0001	
Distance	1	0.2131	0.0338	0.6770	0.3429	0.1440	0.0156	
Slope	1	0.0003	0.0070	0.7948	0.7833	0.9550	0.1448	
Chara	1	0.1771	0.0053	0.8151	0.1092	0.0340	0.0317	
$N + E$[§]	2	<0.0001	<0.0001	0.0099	0.7166	0.4437	0.1215	

$ df = degrees of freedom. § Joint test of northings and eastings.

Parameter estimates for fixed effects in selected models are given in Table 5. Between the estimated parameters, some common patterns could be detected concerning the composition of significant explanatory variables. For example, Calcite corresponded to Can, the Corg content corresponded to S except for the variable of Slope, and Claymin corresponded to MEANTOT, with the exception of Slope and E′. Considering the total variance explained by the model (Table 6), the parameters were grouped into 3 classes:

(1) Parameters with less than 10% *VE*, such as Dolomite, Feldspar, Corg, PCLT63, and MEANLT63 were not represented well by the model and were not described in detail.
(2) Parameters reaching *VE* 10–30% were partly represented by the model, but major explanatory variables seem to be lacking in the model, e.g., for the response variables log(C/D), Quartz, Pyrite, and MEANTOT.
(3) Parameters reaching *VE* > 30%, such as Calcite, Claymin, S, and Can were represented best by the model.

Calcite content increased with depth, distance from shore and Chara density, and decreased with sediment slope (Table 5). Spatial trends were given by the terms α and E′. The rotation angle was $\alpha = -0.77$, which is close to zero, and the slope for E′ was negative so the major trend of calcite content was upward from east to west. Thus, the geographical trend basically followed the flow of water, as the main tributaries enter the lake in the eastern part and the outflow is located in the west part of the lake. The east-west trend, with higher calcite contents in the west, is clearly shown at 4 m water depth and below (Fig. 2), whereas in more shallow sites this trend is not obvious. Although the content of calcite increased with depth and distance from shore, *EFD* was not significant in contributing to the explained variance. The model predicted the calcite content by the following equation (Table 4):

$$\begin{aligned}\text{Calcite (\%)} = {} & 42.48 + 1.18\ \text{Depth (m)} \\ & + 0.82\ \text{Distance (m)} - 0.21\ \text{Slope} \\ & + 5.61\ \textit{Chara} - 0.5482\ \text{E}'\end{aligned}$$

Table 5. Parameter estimates for fixed effects in selected model for variance-covariance models selected for t_i in Table 3.

Term	Calcite	Dolomite	log(C/D)	Quartz	Feldspar	Claymin	Pyrite
Intercept	42.48	2.536	1.814	3.046	1.611	5.275	0.2409
EFD	–	–	–	0.006251	–	0.04800	–
Depth	1.180	–0.02329	0.0457	–0.03185	–	–0.07621	0.007138
Distance (m)	0.8203	–0.03014	0.07120	–0.02673	–	–0.05893	–0.00403
Slope	–0.2173	–	–	0.01319	–	0.01262	–
Chara	5.6076	–	–	–	–	–0.4582	–
E'	–0.5482	–0.03503	–0.03926	0.02544	–	0.02777	–0.002134
α	11.66	–76.17	81.96	11.57	–	41.54	83.42

Term	S	Can	Corg	PCLT63	MEANLT63	MEANTOT
Intercept	–1.840	2.415	1.379	1.703	3.948	5.763
EFD	–0.02958	–	0.01831	–0.04077	–0.02841	0.02348
Depth	0.03147	0.02684	–0.02576	0.05406	–0.03508	–0.07763
Distance (m)	–	0.01720	–	–	0.2359	–0.04296
Slope	–0.01259	–0.00600	–	–	–	–
Chara	–	0.1449	–	–	–	–0.1761
E'	–0.01560	–0.01447	–0.005517	–	–	–
α	51.25	–1.513	–11.98	–	–	–

Table 6. Variance component estimates in selected model with regressors and model without regressors (intercept only model) for variance-covariance models selected for t_i in Table 3.

Parameter/ Statistic	Calcite	Dolomite	log(C/D)	Quartz	Feldspar	Claymin	Pyrite
σ_t^2 (with)	97.79	0.2189	0.04609	0.2209	–	0.2438	0.001203
σ_e^2 (with)	182.51	0.2801	0.05508	0.2884	–	0.8685	0.008125
σ_t^2 (without)	213.55	0.2312	0.05764	0.3769	0.04184	0.7710	0.002144
σ_e^2 (without)	206.62	0.2894	0.06028	0.3065	0.06694	0.9422	0.008441
VE_t	54.20	5.32	20.04	41.39	–	68.38	43.89
VE_e	11.67	3.21	8.63	5.905	–	7.82	3.74
VE	33.29	4.15	14.20	25.48	0	35.07	11.88

Parameter/ Statistic	S	Can	Corg	PCLT63	MEANLT63	MEANTOT
σ_t^2 (with)	0.07634	0.04534	0.02027	0.1229	0.1011	0.09448
σ_e^2 (with)	0.2929	0.08901	0.09022	0.3368	0.4409	0.2875
σ_t^2 (without)	0.2404	0.1151	0.02600	0.1508	0.1331	0.09376
σ_e^2 (without)	0.3045	0.1046	0.09627	0.3529	0.4522	0.3572
VE_t	68.24	60.61	22.04	18.50	24.04	0
VE_e	3.81	14.90	6.28	4.56	2.50	19.51
VE	32.24	38.85	9.63	8.74	7.40	15.30

The regression model explained 33% of the total variance (Table 5), indicating that 67% of the variance remained unexplained. The VE_t value (54.2%) was much higher than the VE_e value (11.7%), thus the model explained much better the between-transect variance than the within-transect variance. A plot of observed versus predicted values for calcite (Fig. 3) showed numerous "outliers", for which the observed values were much less than the predicted. A map of the residuals that differed more than 20% from the observed values suggested that these sample sites were situated in close proximity to shore constructions. This finding indicates that some disturbance of sediments occurred due to construction works in shore areas.

The log (C/D) is a combined parameter of Calcite and Dolomite; the *VE* value of the model was in between the values of these parameters. Because of the very low *VE* value of Dolomite, it was much less than that of Calcite. The model of quartz retained all variables except *Chara*. Explaining 25.5% of the total variance, quartz content in-

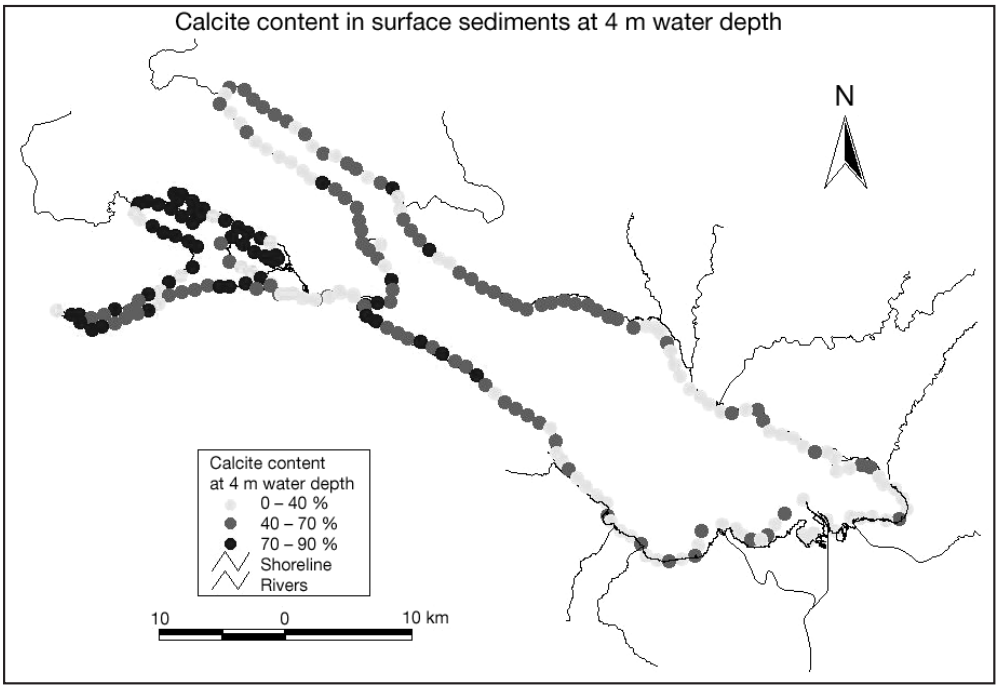

Figure 2. Spatial pattern of calcite content at 4 m water depth in littoral surface sediments of Lake Constance.

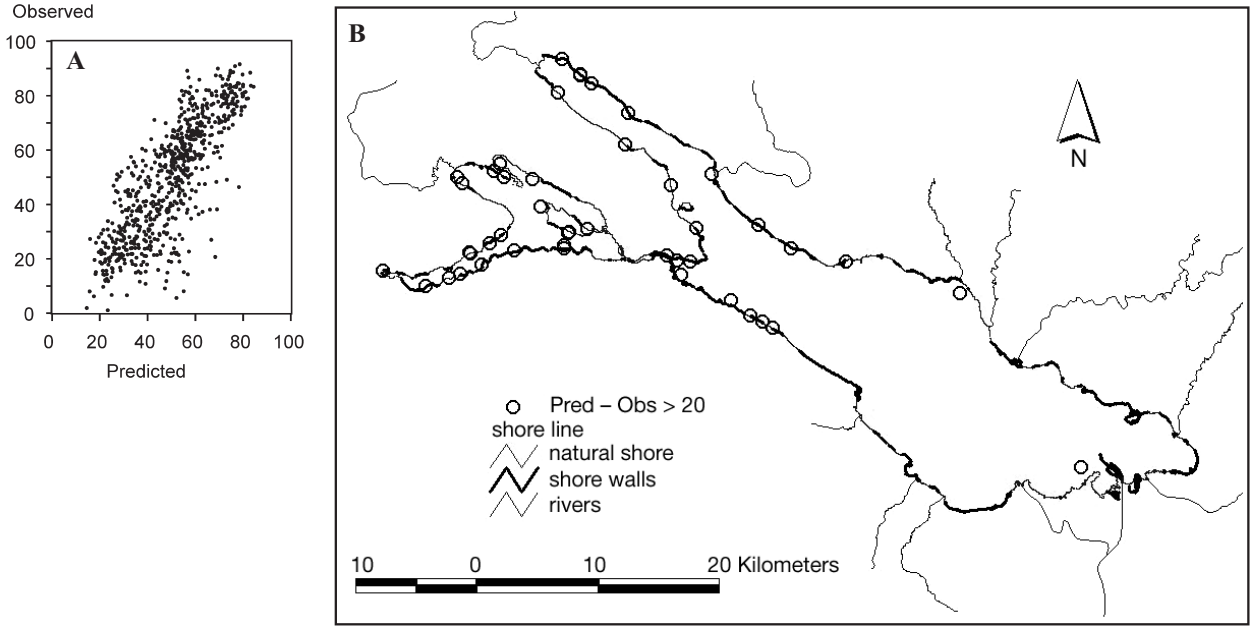

Figure 3. A. Plot of observed versus predicted values for calcite content with the 3-variable model (n = 762).
B. Map indicating the location of sample points where the difference between predicted and observed values constitutes more than 20%.

creased with *EFD* and Slope, but decreased with water depth and distance from shore. The spatial trend in quartz content was opposite to that of calcite, showing concentrations decreasing from east to west. Clay mineral content (Claymin) increased with *EFD*, Slope and from west to east, but decreased with water depth, distance from shore and *Chara* abundance. The spatial trend is therefore similar to that of Quartz. The model explained more than 35% of the variance in Claymin. The VE_t value of 68.4% was the highest found for all models used. Pyrite content increased with water depth and decreased with distance from shore and from north to south. The spatial trend is

similar to that of log (C/D) and opposite to that of Dolomite. Sulphur (S) content increased with water depth and decreased with all other variables retained in the model, such as *EFD*, Slope and E′. The rotation angle was 51°, indicating that the spatial trend in S content was downward in a northwest – southeast direction. Sulphur belongs to the group of four variables best explained by the model. The VE_t value was the second highest obtained in this study. The content of inorganic carbon (Can) increased with water depth, distance from shore and *Chara* abundance, but decreased with slope and from west to east. The rotation angle was –2°, which means a downward trend from west to east. With approximately 39% of the total variance explained, Can was the sediment constituent that was best described by the model. Similar to calcite content, the VE_e value of inorganic carbon content was relatively high compared to other parameters, whereas the VE_t value was lower than that of other parameters, for which a higher percentage of variance was explained by the model, e.g. Claymin and S. Mean total grain size (MEANTOT) was the granulometric parameter best explained by the model. MEANTOT increased with *EFD*, but decreased with water depth, distance from shore and *Chara* abundance. MEANTOT was the only parameter for which the VE_e value contributed more to *VE* than VE_t. The variance within transects was therefore better explained by the model than the variance between transects. However, with a *VE* value of 15.3%, the explained variance of the data was relatively low. For all other parameters VE_t values were much higher than the VE_e, approaching 70% in the case of Claymin and S. This result indicates that the model represents the spatial trends much better than the vertical trends.

Discussion

Our results showed that the explanatory variables relating to geography, lake morphometry and limnology explain up to 30–40% of the total variance of specific components of the littoral surface sediments of Lake Constance. The proportion of the explained between-transect variance (VE_t) contributed much more to the total variance explained by the model than the variance within transects (VE_e). Regional patterns in sediment composition, such as the observed east-west gradient, are therefore much better represented by model variables than local patterns, e.g. the gradient along transect depth. Sediment composition apparently showed no significant continuous gradient with increasing water depth along transects except for the one in mean total grain size. Even for this parameter, the VE_e did not exceed 20%. This result indicates that the applicability of models, developed under an ideal framework (e.g. Petticrew and Kalff, 1991), is limited for the explanation of lake specific spatial patterns. Nevertheless, water depth contributed significantly to most models.

Endogenic processes can explain the pronounced west-east gradient found in calcite contents. The production of endogenic materials, particularly biogenic carbonate, is relatively low in the eastern part of the Upper Lake because few plants grow in this area, as evidenced by long-term patterns in macrophyte distribution (Schmieder, 1997; 1998). Allogenic detrital sources from tributaries are mainly located in the eastern part of the lake. However, they do not contribute substantially to a higher proportion of calcite in littoral sediments of the eastern part of the lake. The higher calcite concentrations in the Lower Lake and the western part of the Upper Lake likely reflect biogenically induced carbonate production. In particular, Charophytes seem to be a significant internal source of sediments in the western part of the lake, as suggested by the significant contribution of the *Chara* abundance to the model and its long-term distribution patterns (Schmieder, 1997; 1998; Schmieder and Lehmann, 2004). Similarly, Schröder (1982) found that Charophytes play a major role in sediment accretion in the littoral zone of Atter Lake. Particularly in the Lower Lake, littoral biogenic carbonate sediments can reach a thickness of several meters (Schöttle, 1969). Sediment calcite content increased with water depth and distance from shore, and decreased with sediment slope. This finding suggests a wave-induced transport of biogenic carbonate particles from more shallow littoral areas to deeper parts of the lake. The most abundant Charophyte, *Chara contraria*, mainly grows between 1 and 4 m water depth (Schmieder, 1997). A permanent relocation of biogenic carbonates from the "productive" sublittoral to deeper parts of a lake has previously been reported (Schröder, 1982). Accumulation of precipitate minerals takes place under relatively static conditions (Jones and Bowser, 1978). Carbonate particles are lighter and more fragile than quartz particles of the same size, and thus are transported alongshore or cross shore to sites with lower influence of currents and waves. However, the *EFD* variable was not significant in our models, and indicates that the offshore transport of carbonates is a general process and not dependent on the predominant strong wind direction from the southwest.

The model of calcite content corresponds closely to that of inorganic Carbon (Can). This result supports the assumption that Can is mainly a measurement of $CaCO_3$. Sulphur (S) content increased with water depth and decreased with all other variables retained in the model, such as *EFD*, Slope and E′. The spatial trend in S content was downward in a northwest – southeast direction, and mainly followed the gradient in macrophyte biomass. The S content is closely related to inorganic carbon, indicating that it is of biogenic origin as well. Variables retained in the model indicate also the sensitivity of organic matter to wave induced transport, which is higher in the eastern part

of the lake and promotes organic decay in protected littoral areas or deeper parts of the lake.

The quartz and the clay mineral content of the sediment decreased with water depth. These two components apparently constitute most of the surface sediments in shallow parts of the littoral zone. Quartz and clay particles seem to be more resistant to erosion (Hjülström, 1935; Jones and Bowser, 1978). The spatial trend of both quartz and clay mineral content, with decreasing concentrations from east to west, is almost opposite to the pattern found for calcite. Both quartz and clay represent allogenic minerals and reflect the geology of the catchment area. The main tributaries enter the eastern part of the Upper Lake. Thus, the load of allogenic components is high in this part of the lake and causes a "dilution" of endogenic sediment components (Müller, 1966a; 1971). In addition, due to the form of the lake basin, fetch distances are generally larger in the eastern part, and transport processes therefore exert more influence on littoral sediment composition.

The east-west gradients in mineralogical parameters are most obvious at water depths of 4 and 8 m (Schmieder, 1998), whereas sediments are strongly affected by wave action in more shallow waters. The allogenic fraction can be considered to reflect primarily physical factors (erosion and transport), whereas the endogenic and authigenic fractions reflect principally chemical factors in lake systems (Jones and Bowser, 1978). Thus, the eastern part of Lake Constance is dominated by physical factors, whereas chemical factors contribute mainly to sediment composition in the western part. Another factor affecting regional patterns in sediment distribution is disturbance by shore construction that often introduces foreign materials into the lake. This effect could be the main reason for the relatively low percentage of explained variance in models for some of the mineralogical parameters.

For mean total grain size, the high percentage of explained within-transect variance is related to the strong influence of *EFD*, water depth and slope on the sediment grain size distribution in the littoral zone. Generally, wave action induces a sorting process of littoral surface sediments resulting in a typical "offshore fining" (Müller, 1966a; Sly 1978). However, our model does not explain any regional patterns in mean total grain size ($VE_t = 0$). This result indicates that the above sorting effect of waves occurs under a range of wave action forces, and is not restricted to shore areas exposed to the main direction of strong winds. The mean total grain size decreases with *Chara* abundance. This finding is not surprising because dense stands of *Chara* are known to lift the turbulent shear stress above the sediment surface, thereby trapping settled material (Vermaat et al., 2000). Furthermore, lake areas with extensive macrophyte beds retain fine-grained sediments over long periods of time (Schröder, 1988). Sedimentation within macrophyte beds has been suggested as an important source of nutrients (Barko et al., 1991; Petticrew and Kalff, 1992; Barko and James, 1997) that stimulate macrophyte growth, and in turn increase sedimentation rates. This positive feedback mechanism often increases the colonisable surface area for macrophytes (Carpenter, 1981). Macrophyte presence or absence is therefore another factor in the littoral sediment prediction model proposed by Petticrew and Kalff (1991). These authors found a high coefficient of determination ($r2 = 0.67$) for a linear regression model with the five explanatory variables fetch, depth, slope, plant presence, and organic matter when predicting the percentage of clay content of littoral sediments. This value is considerably higher than the 35% of explained variance in clay mineral content by our model. One reason for this discrepancy is presumably the design of each study. The authors above preselected a few spatially independent sample locations using map criteria of fetch, depth and bottom slope that represented a wide range in each variable in three categories (low, medium, high), whereas the present study is based on a large data set including all local variations of littoral sediment composition, and allowing for spatial autocorrelation between samples to reveal spatial characteristics in sediment composition, and factors and processes of influence.

Furthermore, the relatively low explained variance compared to Petticrew and Kalff (1991) indicates that sediments represented in our dataset are additionally affected by other factors not represented in these models, such as anthropogenic interference in near shore littoral areas. Another factor not accounted for in our models that likely affects littoral sediment composition is the influence of tributaries; the effect of which depends on their load of suspended solids and the area of distribution in the littoral zone. The tested variable "distance to river mouth" revealed no significance in the modelling procedure. Each tributary entering Lake Constance has its own, specific characteristic that makes it difficult to include their influence as a single variable in a model.

While the major factors contributing to littoral sediment composition found in previous studies are confirmed here, our results show that their explanatory power for spatial patterns of a specific lake will be weak if respective spatial patterns of influencing factors are not taken into account. An example is the exemption from most of the general spatial patterns in sediment composition in the bay of Friedrichshafen where three rivers enter the lake. The bay is exposed to the highest fetch distances measured in Lake Constance. Nevertheless, the grain size means of the bay do not exceed 330 µm even in the shallowest parts. However, the sediment sorting process due to wave action described above also depends on the continuous delivery of allogenic sediments and factors that affect the erosion potential of waves. The tributary "Schussen" entering the bay of Friedrichshafen contains

high amounts (100 mg L^{-1}) of fine sediment particles (Wagner and Zahner, 1964; Wagner, 1968). Every year 30,000–50,000 t of suspended material are widely distributed in the littoral area of the bay (Walser, 1995).

The present study confirms the major factors contributing to littoral sediment composition found in previous studies. However, their explanatory power for spatial patterns of a specific lake will be weak if respective spatial patterns of influencing factors are neglected. The presented model provides a solution to this problem and its application to Lake Constance improves the understanding of spatial patterns of littoral sediment composition and the contribution of allogenic and endogenic sources and processes. It provides a guide to future sampling schemes and corresponding spatial statistics for lake specific application of general models. Furthermore, it provides a guide to generating a basis to support engineering decisions for specific lake development.

Acknowledgments

We wish to thank B. Schuenemann for the performance of the sediment analyses. Special thanks to A. Lehmann for disposing the script for calculating *EFD* in Arcview and to W. Jansen for reviewing the manuscript and improving the English. Financial support of the International Commission for Water Protection of Lake Constance (IGKB) and European Community (Interreg I) is gratefully acknowledged.

References

Barko, J. W., D. Gunnison and S. R. Carpenter, 1991. Sediment interactions with submersed macrophyte growth and community dynamics. Aquat. Bot. **41:** 41–65.

Barko, J. W. and F. James, 1997. Effects of submersed macrophytes on nutrient dynamics, sedimentation and resuspension. In: E. Jeppesen, M. Sondergaard, M. Sondergaard and K. Christoffersen (eds.), The Structuring Role of Submersed Macrophytes in Lakes, Springer Verlag, Berlin, pp. 397–407.

Braun, E. and K. Schärpf, 1994. Internationale Bodenseetiefenvermessung 1990. Landesvermessungsamt Baden-Württemberg, pp. 98.

Brown, B. E., J. L. Fassbender and R. Winkler, 1992. Carbonate production and sediment transport in a marl lake of southeastern Wisconsin. Limnol. Oceanogr. **37:** 184–191.

Carpenter, S. R., 1981. Submersed vegetation: an internal factor in lake ecosystem succession. Am. Nat. **118:** 372–383.

Folk, R. L. and W. C. Ward, 1957. Brazors river bar: a study in the significance of grain size parameters. J. Sediment. Petrol. **27:** 3–26.

Hakanson, L. and M. Jansson, 1983. Principles of Lake Sedimentology. Springer, 316 pp.

Hjülström, F., 1935. Studies of the morphological activities of rivers as illustrated by the river. Fyris Bull. of the Geol. Institute, University of Uppsala **25:** 221–527.

James, F. and J. W. Barko, 1990. Macrophyte influences on the zonation of sediment accretion and composition in a north-temperate reservoir. Arch. Hydrobiol. **120:** 129–142.

Jones, B. F. and C. J. Bowser, 1978. The mineralogy and related chemistry of lake sediments. In: A. Lerman (ed.) Lakes, Chemistry Geology Physics, Springer Verlag, New York, Heidelberg, Berlin, pp. 179–227.

Kelts, K. and K. J. Hsü, 1978. Freshwater Carbonate Sedimentation. In: A. Lerman (ed.) Lakes, Chemistry Geology Physics, Springer Verlag, New York, Heidelberg, Berlin, pp. 295–321.

Küchler-Krischun, J., 1989. Nukleierung der Calcit-Fällung im Bodensee durch Phytoplanktonalgen. Diss., Univ. Konstanz.

Lehmann, A., 1998. GIS modeling of submerged macrophyte distribution using Generalized Additive Models. Plant Ecol. **139:** 113–124.

Littell, R. C., G. A. Milliken, W. W. Stroup and R. D. Wolfinger, 1996. SAS system for mixed models. SAS Institute, Cary.

Mühleisen, R., 1977. Starke Winde an und auf dem Bodensee. Meteorol. Rdsch. **30:** 15–22.

Müller, G., 1966a. Die Sedimentbildung im Bodensee. Naturwissenschaften **53:** 237–247.

Müller, G., 1966b. Methods in sedimentary petrology. E. Schweizerbart'sche Verlagsbuchhandlung (Nägele u. Obermiller), 283 pp.

Müller, G., 1971. Sediments of Lake Constance. In: G. Müller [ed.], Sedimentology of parts of Central Europe, Kramer, pp. 237–252.

Petticrew, E. L. and J. Kalff, 1991. Predictions of surficial sediment composition in the littoral zone of lakes. Limnol. Oceanogr. **36:** 384–392.

Petticrew, E. L. and J. Kalff, 1992. Water flow and clay retention in submerged macrophyte beds. Can. J. Fish. Aquat. Sci. **49:** 2483–2489.

Schmieder, K., 1997. Littoral zone – GIS of Lake Constance: a useful tool in lake monitoring and autecological studies with submerged macrophytes. Aquat. Bot. **58:** 333–346.

Schmieder, K., 1998. Submerse Makrophyten der Litoralzone des Bodensees 1993 im Vergleich mit 1978 und 1967. Ber. Int. Gewässerschutzkomm. Bodensee **46**, 171 pp.

Schmieder, K. and A. Lehmann, 2004. Setting a spatio-temporal framework for efficient inventories of natural resources: a case study with submersed macrophytes in Lake Constance (Germany). J. Veg. Sci. **15:** 807–816.

Schmieder, K., B. Schünemann and H. G. Schröder, 2004. Spatial patterns of surface sediment variables in the littoral zone of Lake Constance (Germany). Arch. Hydrobiol. **161 (4):** 455–468.

Schöttle, M., 1969. Die Sedimente des Gnadensees. Arch. Hydrobiol./ Suppl. **35:** 255–308.

Schröder, H. G., 1982. Biogene, benthische Entkalkung als Beitrag zur Genese limnischer Sedimente. Beispiel: Attersee (Salzkammergut; Oberösterreich). Ph. D. Thesis Univ. of Göttingen, 177 pp.

Schröder, R., 1988. Die Erosion der Uferbank des Untersees (Bodensee). Spätfolgen der Eutrophierung und hydrologischer Phaenomene. Arch. Hydrobiol. **112:** 265–277.

Sly, P. G., 1978. Sedimentary processes in lakes. In: A. Lerman (ed.) Lakes, Chemistry Geology Physics, Springer Verlag, New York, Heidelberg, Berlin, pp. 65–84.

Vermaat, J. E., L. Santamaria and P. J. Roos, 2000. Water flow across and sediment trapping in submerged macrophyte beds of contrasting growth form. Arch. Hydrobiol. **148:** 549–562.

Wagner, G., 1968. Petrographische, mineralogische und chemische Untersuchungen an Sedimenten in den Deltabereichen von Schussen und Argen. Schweiz. Z. Hydrol. **30:** 76–137.

Wagner, G. and R. Zahner, 1964. Die Abwasserbelastung der Uferzone des Bodensees. Ber. Int. Gewässerschutzkomm. Bodensee **2:** 76 pp.

Walser, R., 1995. Zur Rolle der Makrophytenbestände im Bereich von Flussmündungen am Bodensee-Obersee. Ph. D. Thesis Univ. of Hohenheim, 202 pp.

Wolfinger, R. D., 1996. Heterogeneous variance-covariance structures for repeated measures. Journal of Agricultural, Biological and Environmental Statistics **1:** 205–230.